Results from VENUS

K. Ogawa
(VENUS Collaboration)

National Laboratory for High Energy Physics
Oho, Tsukuba-shi, Ibaraki-ken, 305 Japan

Abstract

Recent results from VENUS experiments on e^+e^- reactions at energies between 52 and 60.8 GeV are presented. The R-values, the ratio of the total hadronic cross section to that of μ pair production, look slightly high within the present energy region. To understand this observation, a detailed study was carried out on the production of a heavy quark with $\mid Q \mid$=e/3. By using a next-to-leading log. approximation, the QCD cut-off parameter, $\Lambda_{\overline{MS}}$, was obtained as being $\Lambda_{\overline{MS}}$ =208 $\mathrm{MeV}^{+80MeV}_{-62MeV}$. The differential cross sections for $e^+e^- \rightarrow e^+e^-, \gamma\gamma, \mu^+\mu^-$, and $\tau^+\tau^-$ were found to be consistent with predictions of the standard model. The average charge asymmetry for $e^+e^- \rightarrow q\bar{q}$ was also measured and found to be consistent with the prediction of the standard model. No evidence was observed indicating new particle production. No single photon production was observed and the upper limit of the number of light neutrino types was set to be $N_\nu < 17.8$(90 % CL).

1. Introduction

Since the commissioning run of TRISTAN e^+e^- collider on November 1986, the VENUS[1] detector has been operated stably for about two and a half years. We have accumulated about 25 pb^{-1} of data with energies between 52 and 60.8 GeV. The present talk is based on an analysis of the above-mentioned data, covering the following topics:(1) results on multihadron production, (2) tests of QED and electroweak interactions, (3) the search for new particles, and (4) the search for single photons.

2. Results on Multihadron Production

2-1) Total Cross Section

The R-ratio, the ratio of the total hadronic cross section to that of the lowest-order QED cross section of μ pair production, is used for a search for new heavy quarks, such as the top quark($|Q| = \frac{2}{3}e$) and the b' quark($|Q| = \frac{1}{3}e$). R is evaluated as

$$R = \frac{N_h - N_{bg}}{\epsilon(1+\delta)L\sigma_{\mu\mu}},$$

where N_h is the number of the observed hadronic events, N_{bg} the number of background events, ϵ the acceptance, δ the radiative correction, L the integrated luminosity, and $\sigma_{\mu\mu}$ the calculated lowest-order QED cross section of μ pair production. The rise in R is expected to be 1.36 and 0.44 for full open top and b' production, respectively.

The hadronic event selection criteria is as follows(hereafter, we call this selection criteria the standard selection): (1) The total energy deposited in the calorimeter(the sum of the total energy in the leadglass(LG) calorimeter and liquid argon calorimeter(LA) with $|cos\theta| < 0.9$) is greater than 5 GeV. (2)At least 5 charged tracks are found in the central drift chamber(CDC) within the angular range $|cos\theta| < 0.85$. (3) The visible energy E_{vis}(defined as the sum of the absolute momentum of charged tracks and energy deposited in the calorimeter) is greater than the beam energy. (4) The absolute value of the longitudinal momentum balance(defined as the sum of the projected momentum and energy on the beam axis) is less than $0.4 \times E_{vis}$. The detection efficiency was determined by Monte Carlo simulation, where events were generated based on the standard electroweak theory[2] and subsequent quark fragmentation and QCD correction were simulated by the Lund5.3 program[3]. The radiative effect was corrected based on a calculation by Fujimoto and Shimizu[4].

The systematic errors of R consist of (1) a systematic error of luminosity, 2.6%; (2) errors in radiative correction, 2.1 %; (3) errors due to Monte Carlo parameters and hadronization model, 1.6%; (4) errors in calculating the acceptance, 1.8%; and (5) background contamination, 0.2%. The total systematic error was found to be 4.2% by adding the above errors in quadrature.

The obtained R-values are shown in Fig. 1. The solid curve in the figure is a prediction of the standard model[2] with the Z_0 mass of 92.5 GeV and $sin^2\theta_w$=0.226. The expectation values for full open top and b' production are also given in the figure as dashed and dot-dash curves, respectively. From the figure we can exclude open top production at the present energy. It is, however, interesting that the measured R's are systematically high by about 8% compared to the prediction of the standard model with energies above 56 GeV. They lie just on the expected line of full open b' production. This interesting problem will be discussed later. We will first give the mass limit of the top quark by shape analysis.

2.2) Search for a Top Quark

As has been seen regarding the R-values, open top quark production is unlikely. The mass limit of the top quark will be obtained by event shape analysis. A Q-plot for data at $\sqrt{s}$=60.8 GeV and top quark production with m_t=28 GeV is given in Figs. 2(a) and 2(b), respectively. Q_i(i=1,2,3) is the eigenvalue of the spherical tensor. We observed 5 events in the spherical region defined by $Q_1 > 0.05$ and $(Q_3 - Q_2)/\sqrt{3} < 0.4$. By comparing the above events with the expectation from top-quark production, we could set the lower limit of the top-quark mass at 29.0 GeV at a 95 % confidence level.

2-3) Search for b' Quark

As stated before, the measured R's are slightly higher than the predictions of the standard model and are consistent with full open b' production. Is R really high, indicating open b' production or a new physics? We should at first point out the following fact. If we consider systematic errors, we cannot say that the present rise in R is significant. It is easy to see this by considering that systematic errors should be added linearly. The linear addition of the systematic error(4.2%) and statistical error($\sim$4%) leads to a total error of about 8%, which agrees with the amount of rise in R. This means that the measured R's are consistent with the prediction of the standard model. The same thing can be expressed by the Z^0 mass. The Z^0 mass obtained by fitting the R's is M_z=$88.9^{+1.5+2.5+0.4}_{-1.3-2.3-0.4}$ GeV, where $sin^2\theta_w$ is calculated by the Z^0 mass using the following relation :

$$sin^2\theta_w = \frac{1}{2}\left[\ 1 - \sqrt{1 - \frac{4\pi\alpha}{\sqrt{2}G_F M_z^2(1-\Delta r)}}\ \right].$$

The errors in the Z^0 mass are (in order): statistical, systematic, and theoretical (which results from errors in QCD parameters and a radiative correction). Though the center value for the Z^0 mass is low, it is consistent with the predicted value by the standard model within the present errors if they are added linearly.

We have seen so far that a search for the b' quark only from R is difficult at this statistical level. The search for the b' quark can be efficiently carried out by looking into the detailed event signatures characteristic to b' production. In the following

section we present a systematic study of b' production

In the search for the b' quark we should study two kinds of decay modes:(1) decay via a charged current(CC) and (2) decay via a loop-induced flavour-changing neutral current(FCNC)[5].

The event signature of the CC decay mode is either isolated lepton or spherical events(3-body decay) via virtual W decay. As for the FCNC decay mode, the event signature is either an isolated photon or spherical events(4-jet).

2-3-1) CC decay mode of b' quark

a) Isolated Lepton

Because prompt leptons coming directly from the decay of heavy quarks have a higher momentum than those from the 5 flavour quarks and are often isolated from jets, we can detect heavy quarks by tagging these isolated leptons. Events were selected by the criteria that (1) it is a standard hadronic event, (2) the thrust is less than 0.9, and (3) at least one isolated lepton exists. An isolated lepton in the present analysis is defined as:

(a) The momentum of leptons is greater than 4 GeV/c.

(b) The energy flow (E_{flow}) within a 30°-cone around the lepton is less than 1 GeV.

The analysis is based on a data sample of 17.7 and 18.2 pb^{-1} with energies between 56 and 60.8 GeV for muon and electron channels, respectively.

Muon Channel

At first, we present an analysis of isolated muon events. A muon is identified by the matching of tracks in CDC and the muon chamber. A detection efficiency of 91.9 $\pm$0.9% was obtained by a cosmic-ray test. In Figs.3(a) and 3(b), a scatter plot of hadron events including muons is shown for energies above 60 GeV(5.9 pb^{-1}) and below 60 GeV(11.8 pb^{-1}), respectively. The horizontal axis is the muon momentum and the vertical axis, the isolation angle θ_c(the maximum angle where E_{flow} within that cone is less than 1 GeV). We have observed 3 isolated muon events with energies above 60 GeV, and no events below 60 GeV. The expected number of events from 5f and $\tau\tau$, and two-photon process is 0.26$\pm$0.04 for energies above 60 GeV. Therefore, if Monte Carlo simulation is reliable, it is difficult to explain the observed 3 events by the known processes. Does this indicate some new physics? A check of the energy dependence of the observed data provides a Monte-Carlo-independent test. We compared the observed events above and blow 60 GeV by carrying out F test[6] where we assumed that both events were produced according to the same Poisson distribution. The probability that isolated muon events above and below 60 GeV came from the same Poisson distribution is less than 1%. This is an interesting result. One explanation of this observation may be b' production. The expected number of events from b' production with $m_{b'}$ around 28 GeV is consistent with the observed events. If this is true we can expect the same number of isolated electron events. In the next section, we present an analysis of an isolated electron.

Electron Channel

Since we observed interesting events in the muon channel, the search for an isolated electron becomes more interesting. The electron was identified by the E/P method, requiring that E/P be between 0.8 and 1.3. The detection efficiency was obtained to be 85±2% for an electron energy greater than 4 GeV. The event-selection criteria are the same as those for the isolated muon events. The results are shown in Figs.4(a) and 4(b), where isolated electron events are plotted against the electron momentum and the isolation angle with energies above 60 GeV(5.9 pb^{-1}) and below 60 GeV(12.3 pb^{-1}), respectively. We have observed 2 isolated electron events with energies above 60 GeV, and no events below 60 GeV. The expected number of events from 5f, $\tau\tau$ and the two-photon process is 0.6±0.1 for energies above 60 GeV. Thus, the observation of 2 isolated electron events is rare if Monte Carlo simulation is reliable. According to the F-test, the probability that events above and below 60 GeV were produced according to the same Poisson distribution is less than 2.5%. The result is again interesting. Together with the isolated muon events, the observed electron events seem to indicate b' production. Now, an analysis of the CC hadronic decay mode of the b' quark is indispensable in the search for b' production. We show the hadronic decay mode in the next section.

b) Hadronic Decay Mode(CC)

In general, the production of a heavy quark near the threshold is characterized by its spherical shape in the final states. In the present study we searched for spherical events with the following selection criteria: (1) it is a standard hadronic event, (2) the absolute value of the longitudinal momentum balance is less than 0.2 × E_{vis}, (3) the thrust is less than 0.75, and (4) the acoplanarity is greater than 0.15. The integrated luminosity of data sample is 18.2 pb^{-1} with energies between 56 and 60.8 GeV. In Figs.5(a) and 5(b), scatter plots of the events are shown for energies above 60 GeV(5.9 pb^{-1}) and below 60 GeV(12.3 pb^{-1}), where the horizontal axis is the thrust and the vertical axis is the acoplanarity. We have observed 8 and 7 events with energies above and below 60 GeV, respectively. Again, we carried out an F test. The probability that the observed events below and above 60 GeV came from the same Poisson distribution is less than 5%. This probability supports the results of isolated-lepton analysis, an indication of b' production above 60 GeV. The expected events from b' production are consistent with the observed events above 60 GeV if $m_{b'}$ is around 28 GeV.

So far, we have studied the charged current decay of the b' quark by observing any excess in isolated lepton events and spherical events. All channels of the CC decay mode of the b' quark indicate its existence. It should, however, be said that the statistical significance is not yet sufficient to conclude b' production. We need at least 5 times more integrated luminosity for a definite conclusion.

2-3-2) FCNC decay mode of b' quark

a) Isolated Photon

As has been pointed out[5], if the b' quark is lighter than the top quark, CC decay is strongly suppressed due to the quark mixing angle. In that case, it is very likely that b' can decay via FCNC into a b quark by emitting either a photon, a gluon, a Z_0, or a neutral Higgs. In the present analysis we studied two cases: b' decaying to $b\gamma$ or bg. First, we show $b' \rightarrow b\gamma$ decay, where the event signature is an energetic isolated photon.

The analysis is based on a data sample of 21.1 pb^{-1} with energies of 55 to 60.8 GeV. The event selection criteria is that: (1) it is a standard hadronic event, and (2) at least one isolated photon exists which satisfies following conditions:

(a) There exists a cluster with $|cos\theta| < 0.685$ with an energy larger than 0.1 times E_{beam}.

(b) There exist no other clusters with an energy exceeding 1 GeV, nor good tracks within a 30° cone around the cluster.

Fig. 6(a) is the energy spectrum of isolated photons. The histogram represents the spectrum of the initial state radiation simulated by the LUND5.3 program with 5 known flavours. The contamination of π^0 was estimated by isolated charged pions and is shown by crosses in Fig.6(a). The agreement between data and expectation by Monte Carlo simulation is excellent. Figure 6(b) shows the photon spectrum expected from the b' quark with masses of 29, 26 and 20 GeV. By cutting the photon spectrum between 0.3 and 0.7 times E_{beam} we obtained 8 events. The expectation from the initial state radiation is 11.0±1.1 and is consistent with our data. Considering both FCNC and CC decay modes, the limits on the mass of the b' quark against the absolute photonic branching ratio were obtained and are shown in Fig.7. At the typical photonic branching ratio of 10%, a b' mass between 13 and 27 GeV is excluded at a 95% confidence level.

b) Hadronic Decay Mode(FCNC)

We add here an analysis of the hadronic decay mode of the b' quark. The event-selection criteria are the same as those adopted in an analysis of the hadronic decay mode in CC. The observed events were compared with the expectation from $b' \rightarrow bg$ decay, where quark and gluon hadronization were simulated by the LUND6.3 program[7]. A b' mass between 18.5 and 25 GeV is excluded at a 100% bg decay branching ratio.

2-4) Determination of $\Lambda_{\overline{MS}}$

The QCD cut-off parameter, Λ_{QCD}, or running coupling constant, α_s, is one of the important parameters in the standard model. So far, α_s has been determined by various methods such as R, Energy-Energy-Correlation, shape variables and so on[8]. In the present analysis, preliminary results on $\Lambda_{\overline{MS}}$ obtained by the 3-jet fraction R_3 is reported. The analysis is based on a standard hadronic data sample of 17 pb^{-1} with energies between 55 and 60 GeV. FiG.8 is the multijet fraction obtained

by the jet clustering algorithm used by JADE collaboration[9]. To obtain the QCD cut-off parameter, quarks and gluons were generated according to the QCD cascade shower based on a next-to-leading log(NLL) approximation[10]. This scheme has the following advantages:(1) the hard 3-jet cross section is correct, and (2) the scheme for QCD Λ is fixed. Thus, the QCD cut-off parameters can be obtained directly by comparing the measured R_3 with the simulated ones for various cut-off parameters. We have obtained cut-off parameter to be $\Lambda_{\overline{MS}} = 208^{+80}_{-62}$ MeV. The corresponding strong coupling constant is $\alpha_s = 0.125 \pm 0.007$ at $< \sqrt{s} >$=57.3 GeV.

3. Test of QED and Electroweak Theory

3-1) $e^+e^- \rightarrow e^+e^-$

Bhabha scattering is of fundamental importance since it provides a good way to test QED and, further, is used to determine the integrated luminosity. Bhabha scattering events were selected by requiring two collinear clusters ($E_{cl} > \frac{1}{3}E_{beam}$, $\theta_{acol} < 10°$) in LG or LA with an association of charged tracks for clusters in LG. The angular distribution of Bhabha events at an energy of 60.8 GeV is shown in Fig.9(a). In Fig.9(b) the total cross section with $cos\theta < 0.743$ is plotted against the center-of-mass energy. The dotted and solid curves in the figures are predictions of QED and the standard model. The data are consistent with the predictions of QED or the standard model. The deviations from QED are parameterized in terms of the cut-off parameters defined by

$$(\frac{d\sigma}{d\Omega})_{exp} = (\frac{d\sigma}{d\Omega})_{EW} \times [1 \mp \frac{3s}{\Lambda_{\pm}^2} \times \frac{1 - cos^2\theta}{3 + cos^2\theta}] \ .$$

The 95% confidence lower limits of cut-off parameters were obtained to be 214 and 506 GeV for Λ_+ and Λ_-, respectively.

3-2) $e^+e^- \rightarrow \gamma\gamma$

The $e^+e^- \rightarrow \gamma\gamma$ process provides a pure test for QED. The event-selection criteria is similar to Bhabha scattering, except that at least one cluster is not associated with a charged track. The angular distribution and total cross section is shown in Figs.10(a) and 10(b) with energies between 55 and 60.8 GeV. The solid curves in the figures are predictions from QED and are consistent with the data.

The QED cut-off parameters defined by

$$(\frac{d\sigma}{d\Omega})_{exp} = (\frac{d\sigma}{d\Omega})_{QED} \times [1 \pm \frac{s^2}{2\Lambda_{\pm}^4} \times sin^2\theta]$$

were obtained to be 95 and 83 GeV for Λ_+ and Λ_-, respectively.

3-3) $e^+e^- \to \mu^+\mu^-/\tau^+\tau^-$

The forward-backward(FB) asymmetry in fermion pair production is important for testing the electroweak theory since the interference between electromagnetic and weak interactions causes a large FB-asymmetry in TRISTAN energy region. In this section FB-asymmetry of μ and τ pair is presented. The Figs.11(a) and 11(b) are the measured angular distribution for μ and τ pair production, respectively. The dashed curves in the figures are the prediction from the standard model with $sin^2\theta_w$=0.226 and M_z=92.5 GeV. The FB-asymmetries can clearly be seen and agree well with predictions of the standard model. The cross section and asymmetry are summarized in table 1.

3-4) The Jet Charge Asymmetry

The FB charge asymmetry in quark pair production is also important for testing the standard model. The charm and bottom quark asymmetry have been measured by tagging these quarks via a semi-leptonic decay of a heavy quark meson or reconstruction of a charm meson[11]. However, measurements are not statistically significant due to the low tagging efficiency. If original quarks cannot be identified, we can measure the average charge asymmetry by determining the original quark charge through a suitably weighted jet charge[12]. This asymmetry is small due to a large cancellation between different quarks, as expressed by

$$A_{jet} = f_d A_d - f_u A_u + f_s A_s - f_c A_c + f_b A_b,$$

where the polar angle θ is taken to be that between an electron and the negatively charged jet.

In the TRISTAN energy region, however, the asymmetry is expected as large as 10%. Here, the preliminary results of jet charge asymmetry is reported. The analysis is based on a hadronic data sample of 24.8 pb^{-1} with energies between 52 and 60.8 GeV. The two jet events were selected with the additional requirement that:(1) the thrust is greater than 0.85, (2) at least two tracks exist in each hemisphere divided by the plain perpendicular to the thrust axis, and (3) at least one jet has a mass higher than 1.78 GeV. The jet charge in each hemisphere is determined by

$$Q_{jet} = \sum q_i \times (\frac{p_i}{E_{beam}})^\alpha \ ,$$

where q_i and p_i are the charge and the momentum of the i'th track. The summation is taken over all charged tracks in each hemisphere. The original quark charge was determined by comparing the jet charge of each hemisphere: if $Q_{jet1} > Q_{jet2}$, then the charge of jet1 was assigned to be positive. The charge identification probability was 71 and 74% for a down-like quark and an up-like quark, respectively. Acceptance and charge misidentification were corrected by the LUND5.3 program. Fig.12 shows the angular distribution of a hadron jet. The charge asymmetry can be clearly seen. The obtained asymmetry is $11.2 \pm 2.5\%$ at 56.8 GeV. The systematic errors

consist of (1)charge misidentification(13.5%), (2) radiative correction(10%), (3)QCD effect(5%) and (4) Monte Carlo errors(5.9%), with a total of 18.5%, corresponding to 2.1 % in asymmetry. The expected value from the standard model is 8.4% when $B^0\overline{B^0}$ mixing is not considered. When $B^0\overline{B^0}$ mixing is considered with mixing parameters of $\chi_d = 0.17 \pm 0.05$[13] and $\chi_s = 0.5 \pm 0.5$, the expected asymmetry is 10.4%. The measured asymmetry is consistent with the prediction of the standard model within the error. We comment that at present we cannot discuss on $B^0\overline{B^0}$ mixing from average charge asymmetry due to large systematic errors.

3-5) Substructure of Quarks and Leptons

The compositeness[14] of quarks and leptons can be studied by investigating the deviation in the differential cross section from that expected from the standard model. We have not observed any deviation or excess in the differential cross section in Bhabha scattering, μ pair production, τ pair production, or quark pair production. Thus, we could place new lower limits on compositeness scale parameters for leptons and quarks(Table 2), where the definition of the compositeness scale parameters is found in ref[15].

4. Search for New Particles

Various new particles, other than heavy quarks, were also searched. So far, no excess has been observed and the mass limits of these particles have been placed. The results are summarized in Table 3.

5. Search for Single Photons

Since the VENUS detector is hermetic with an angular cov ~ge up to $|cos\theta|$ <0.99, we are in good place to search for single photons produced via a radiative production of particles that interact only weakly in matter. One of such reactions is radiative neutrino pair production. Since the cross section of this reaction[16] depends largely on the number of light neutrino types, we can estimate the total number of light neutrino types by serching for single photon events.

The analysis is based on a data sample of 20.3 pb^{-1} with energies between 55 and 60.8 GeV. The events were selected by the following procedure. First, single-photon candidates were selected with the requirement that only one energetic cluster(E_γ >4 GeV) existed in the barrel region($40° < \theta_\gamma < 140°$) without any tracks nor other cluster with energy more than 0.2 GeV. Secondly, the cosmic rays were rejected by the requirement that: (1) no tracks existed in the muon chamber that were connected to the cluster, (2) the timing of the cluster agreed with the beam-crossing time within 5 nsec, (3) when hits in a streamer tube detector and a TOF counter were available, it was checked whether cluster was pointing to the interaction point. Thirdly, the

shower profile of the cluster was checked whether it was consistent with an electromagnetic shower, by making a comparison with the shower profile obtained by the electron beam test. Finally, the QED background which came from $e^+e^- \to ee\gamma/\gamma\gamma\gamma$ with two electrons(gammas) escaping into the beam pipe were rejected by a kinematical constraint expressed as

$$P_t^\gamma/\sqrt{s} > \theta_{veto}.$$

The detection efficiency for single photons is 69.3% for the above selection.

Fig.13(a) shows the $X_t(= P_t^\gamma/E_{beam})$ distribution of single-photon events when θ_{veto} is 15°. The solid line is the expectation from $ee\gamma+\gamma\gamma\gamma$ events where two electrons or gammas escape in a 15°-cone around beam axis. The spectrum agrees well with the prediction. Fig.13(b) shows the single-photon spectrum when a veto angle of 4.4° is imposed. The kinematical limit for $ee\gamma/\gamma\gamma\gamma$ events were set at $X_t > 0.2$ by considering systematic errors. Since we observe no single-photon events above kinematical limit, we can place an upper limit on the number of light neutrino types. The result is $N_\nu < 17.8$ at a 90% confidence level. If we combine the present result with the data from ASP[17], MAC[18], CELLO[19] and MARK-J[20], we obtained an upper limit of N_ν to be $N_\nu < 4.1$ at a 90% confidence level.

6. Conclusion

1. The R-values measured by VENUS look high. However, if we consider systematic errors, the measured R-values are consistent with the prediction of the standard model.
2. No evidence has been observed for open top-quark production. The lower limit for the top-quark mass has been obtained to be $m_t > 29.0$ GeV/c^2 at 95 % CL.
3. We have observed 5 isolated lepton events ($3\mu + 2e$) and 8 spherical events above 60 GeV. The observed events are consistent with the expectation from b' production with $m_{b'}$ around 28 GeV/c^2. However, the statistical significance is still poor.
4. The FCNC decay mode of the b' quark has also been studied by tagging isolated photons. No excess has been observed and the mass limit for the b' quark has been set in this decay mode.
5. Using an NLL approximation, the QCD cut-off parameter $\Lambda_{\overline{MS}}$ has been obtained by R_3. ($\Lambda_{\overline{MS}} = 208^{+80}_{-62}$ MeV.)
6. The $e^+e^- \to e^+e^-, \gamma\gamma$ processes are consistent with the QED prediction.
7. FB asymmetry agrees well with the prediction of the standard model, not only in the lepton channel but also in the quark channel.
8. The lower limits of the compositeness scales for leptons have been updated. The limits are also given for quark compositeness scales.
9. No evidence has been observed for the new particle production. New mass limits have been given.
10. No single-photon events have been observed. The limit for the number of light

neutrino types has been set at $N_\nu < 17.8$ at 90 % CL.

Acknowledgement

The author would like to thank his colleagues in the VENUS group for their help in preparing the present talk. He also acknowledges the organizing committee for inviting him to the conference. The experiments would have been impossible without the skillful operation by TRISTAN machine groups and the invaluable supports by technical staff at KEK and various Universities.

References

[1] The VENUS collaboration
K. Abe, K. Amako, Y. Arai, Y. Asano, M. Chiba, Y. Chiba, M. Daigo, T. Emura, I. Endo, M. Fukawa, T. Fukui, Y. Fukushima, J. Haba, D. Haidt, I. Hayashibara, Y. Hemmi, M. Higuchi, T. Hirose, Y. Hojyo, Y. Homma, Y. Hoshi, Y. Ikegami, N. Ihihara, T. Kamitani, N. Kanematsu, J. Kanzaki, R. Kikuchi, T. Kondo, T. Koseki, K. Kubo, H. Kurashige, T. Matsui, M. Minami, K. Miyake, S. Mori, Y. Nagashima, T. Nakamura, I. Nakano, Y. Narita, S. Odaka, K. Ogawa, T. Ohama, T. Ohsugi, A. Okamoto, A. Ono, H. Osabe, T. Oyama, H. Saito, H. Sakae, H. Sakamoto, S. Sakamoto, M. Sakano, M. Sakuda, N. Sasao, M. Sato, M. Shioden, J. Shirai, F. Suekane, S. Sugimoto, T. Sumiyoshi, Y. Suzuki, Y. Takada, F. Takasaki, A. Takatani, N. Tamura, R. Tanaka, N. Terunuma, K. Tobimatsu, T. Tsuboyama, A. Tsukamoto, S. Uehara, Y. Unno, M. Utsumi, M. Wakai, T. Watanabe, Y. Watase, Y. Yamada, T. Yamagata, T. Yamashita, Y. Yonezawa, and H. Yoshida

[2] S.L.Glashow, Nucl. Phys. 22(1961)579;
A.Salam, Phys. Rev. 127(1962)331;
S.Weinberg, Phys. Rev. Lett. 19(1967)1264.

[3] T.Sjostrand, Comput. Phys. Commun. 27(1982)243.

[4] J.Fujimoto and Y.Shimizu, Mod. Phys. Lett. 3A(1988)581

[5] V. Barger, R.J.N.Phillips and A.Soni, Phys. Rev. Lett. 57(1986)1518;
B.Haeri, A.Soni, and G.Eilam, Phys. Rev. Lett. 62(1989)719;
W.Hou and R.Stuart, Phys. Rev. Lett. 62(1989)617.

[6] D.R.Cox, Biometrica, Vol.40(1953)354

[7] M.Bengtsson and T.Sjostrand, Nucl.Phys. B289(1987)810, and Comput. Phys. Commun. 43(1987)367.

[8] References on measurement of α_s are summarized in the talk by M.Sakuda at the International Conference on Physics in Collision, Capri, Italy, 1988, KEK preprint 88-88(1988).

[9] W.Bartel et al., Z. Phys. C33(1986)23.

[10] K.Kato and T.Munehisa, Phys. Rev. D36(1987)61.

[11] W.Bartel et al., Phys. Lett. 146B(1984)437;
H.J.Behrend et al., Z. Phys. C 19(1983)291;
M.Althoff et al., Z. Phys. C 22(1984)219, and Phys. Lett. 146B(1984)443;
H.Aihara, et al., Z. Phys. C 27(1985)39;
M.Althoff et al., Phys. Lett. 126B(1983)493;
W.Bartel et al., Phys. Lett. 146B(1984)121;
P.Baringer et al., Phys. Lett. 206B(1988)551.

[12] R.D.Field and R.P.Feynman Nucl. Phys. B136(1978)1.

[13] H.Albrecht et al., Phys. Lett. 192B(1987)245.

[14] E.J.Eichten, K.D.Lane and M.E.Peskin, Phys. Rev. Lett. 50(1983)811.

[15] E.J.Eichten, I. Hincliffe, K.D.Lane and C. Quigg Mod. Phys. 56(1984)579.

[16] K.J.F.Gaemers, R.Gastmans, and F.M.Renard, Phys. Rev. D19(1979)1605;
E.Ma, and J.Okada, Phys. Rev. Lett. 41(1986)287.

[17] C.Hearty et al., Phys. Rev. D39(1989)3207.

[18] W. T. Ford, et al., Phys. Rev. D33(1986)3472.

[19] H.J.Behrend et al., Phys.lett. B215(1988)186.

[20] H. Wu, Ph.D. Thesis, Univ. Humburg, 1986.

Table 1 FB Asymmetry and Cross Section of Lepton

Leptons	$\sqrt{s}$	$R_{measured}$	$A_{measured}$
$\mu^+\mu^-$	50-60 GeV	1.06 ± 0.05	-0.283 ± 0.054
$\tau^+\tau^-$	50-60 GeV	1.03 ± 0.07	-0.266 ± 0.073
The standard model	56.1 GeV	1.04	-0.298

Table 2. Lower Limits on Compositeness Scale (95%CL)

Reaction	Compositeness Scale (in TeV)							
	Λ^+_{LL}	Λ^-_{LL}	Λ^+_{RR}	Λ^-_{RR}	Λ^+_{VV}	Λ^-_{VV}	Λ^+_{AA}	Λ^+_{AA}
$e^+e^- \to e^+e^-$	1.2	2.9	1.1	2.8	2.5	5.9	2.3	1.7
$e^+e^- \to \mu^+\mu^-$	1.6	1.8	1.6	1.8	2.8	3.1	2.4	2.8
$e^+e^- \to \tau^+\tau^-$	1.6	1.3	1.6	1.3	3.5	2.2	1.8	3.3
$e^+e^- \to q\bar{q}(*)$	0.9	1.5	1.5	2.2	3.9	2.2	3.4	5.0
$e^+e^- \to q\bar{q}(**)$	0.9	1.5	1.6	1.8	2.9	2.3	3.7	4.0

Reaction	Compositeness Scale (in GeV)							
	Λ^+_{L+R}	Λ^-_{L+R}	$\Lambda^+_{L/R}$	$\Lambda^-_{L/R}$	Λ^+_{L-R}	Λ^-_{L-R}		
$e^+e^- \to \gamma\gamma$	95	83	81	70	59	59		

$*$ without $B^0\overline{B^0}$ mixing

$**$ including effect of $B^0\overline{B^0}$ mixing with $\chi_d = 0.17 \pm 0.05$ and $\chi_s = 0.5 \pm 0.5$

Table 3. List of Mass Limits for Various New Particles

Name of Particle	Mass Limit(95%CL)
Heavy Lepton	$> 29.7 GeV$
Heavy Neutrino	$> 26.8 GeV$
Electron-type Heavy Neutrino	
V+A	$> 51.7 GeV or < 12.5 GeV$
V−A	$> 48.5 GeV or < 17.3 GeV$
Leptoquark(2nd gene.)	
μ s decay	$> 25.4 GeV or < 5.2 GeV$
c ν decay	$> 27.0 GeV or < 8.5 GeV$
Excited Leptons	
e*(from pair production)	$> 30.1 GeV$
e*(from single production)	$> 60.5 GeV$
μ*(from pair production)	$> 30.1 GeV$
μ*(from single production)	$> 53.0 GeV$
τ*(from pair production)	$> 28.0 GeV$
τ*(from single production)	$> 50.0 GeV$
SUSY particles	
$\tilde{e}_L(M_{\tilde{e}_L} = M_{\tilde{e}_R})$	$> 29.5 GeV$
$\tilde{e}_L(M_{\tilde{e}_L} \ll M_{\tilde{e}_R})$	$> 27.5 GeV$
$\tilde{\tau}_L(M_{\tilde{\tau}_L} = M_{\tilde{\tau}_R})$	$> 24.7 GeV$
$\tilde{\tau}_L(M_{\tilde{\tau}_L} \ll M_{\tilde{\tau}_R})$	$> 22.6 GeV$
$\tilde{H}^{\pm}(Br(\tilde{H}^{\pm} \rightarrow \tilde{\tau}\nu)=100\%)$	$> 28.2 GeV$
Scalar Boson	$\Gamma_{ee} <$ a few MeV (for 54 GeV$< M_s < 60 GeV$)

Figure Captions

Fig.1: R vs $\sqrt{s}$. The solid line represents a prediction by the standard model with 5 flavours, where M_z=92.5 GeV, Γ_z=2.5 GeV and $sin\theta_w$=0.226. Dashed and dot-dash curves correspond full open top and b' production.

Fig.2: Q-plot for (a) data at 60.8 GeV and (b) open top production with M_t=28 GeV.

Fig.3: Scatter plot of isolated muon events for (a) energy above 60 GeV and (b) energy below 60 GeV. The horizontal axis is the muon momentum and the vertical axis is the isolation angle.

Fig.4: Scatter plot of isolated electron events for (a) energy above 60 GeV and (b) energy below 60 GeV.

Fig.5: Scatter plot of hadronic events for (a) energy above 60 GeV and (b) energy below 60 GeV. The horizontal axis is the thrust and the vertical axis is the acoplanarity.

Fig.6: (a) Isolated photon spectrum. The solid line represents the initial state radiation simulated by the LUND5.3 program with 5 flavour. The crosses indicate contributions from isolated π^0. (b) Isolated photon spectrum from b' production with $m_{b'}$= 29 GeV(solid line), 26 GeV(dashed line), and 20 GeV(dotted line).

Fig.7: The 95% CL lower limits of the b' quark mass $m_{b'}$ as a function of the photonic branching ratio.

Fig.8: Jet cluster distribution as a function of y_{cut}. Solid lines represent predictions by the NLL approximation.

Fig.9: (a) Differential cross section of Bhabha scattering at $\sqrt{s}$= 60.8 GeV. (b) Total cross section of Bhabha scattering with $|cos\theta| < 0.743$.

Fig.10: (a) Differential cross section of the $e^+e^- \to \gamma\gamma$ process at $< \sqrt{s} >$= 57.2 GeV. (b) Total cross section of the $e^+e^- \to \gamma\gamma$ process with $|cos\theta| < 0.743$.

Fig.11: Differential cross section of (a) $e^+e^- \to \mu^+\mu^-$ and (b) $e^+e^- \to \tau^+\tau^-$. The dashed lines represent predictions of the standard model and the solid lines are fits to data.

Fig.12: Differential cross section of a hadron jet. The dashed line represents a prediction of the standard model and the solid line is a fit to data.

Fig.13: Single-photon spectrum for (a) $\theta_{veto} = 15°$ and (b) $\theta_{veto} = 4.4°$. The solid line represents the single photons from $e^+e^- \to e^+e^-\gamma + \gamma\gamma\gamma$ events.

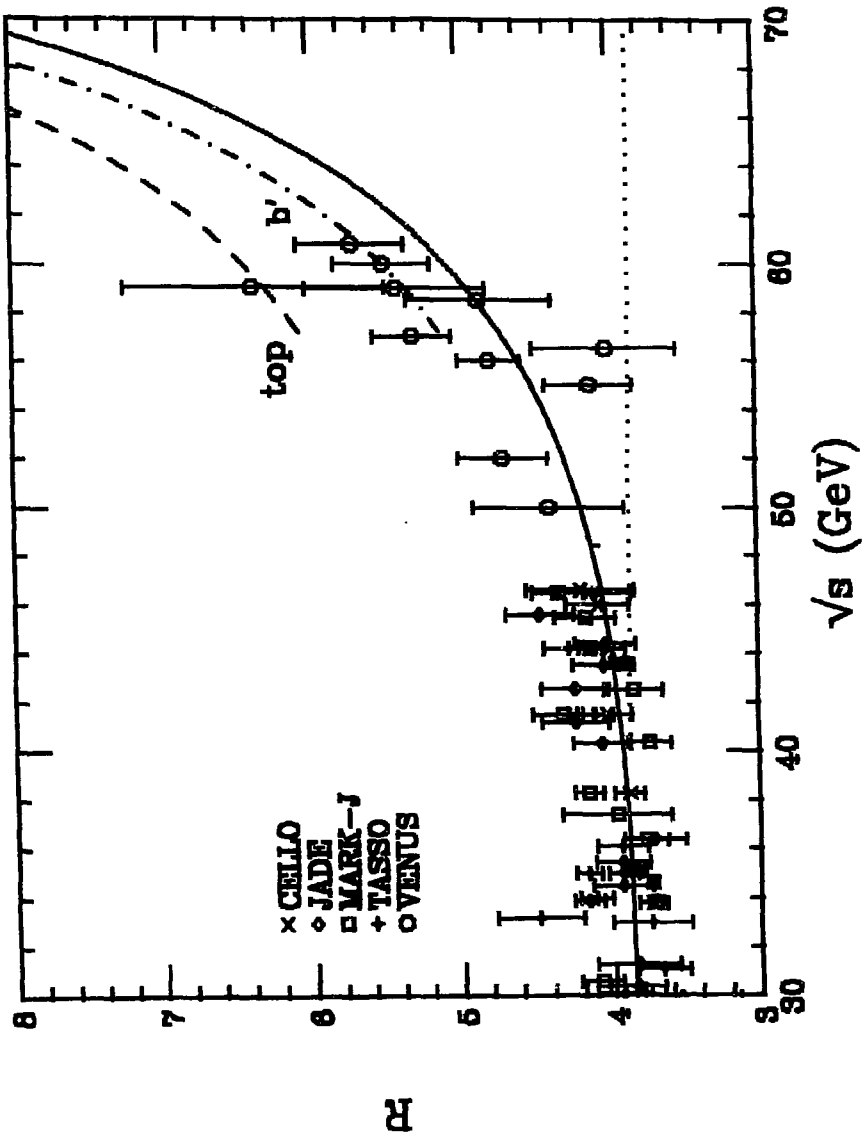

Fig.1

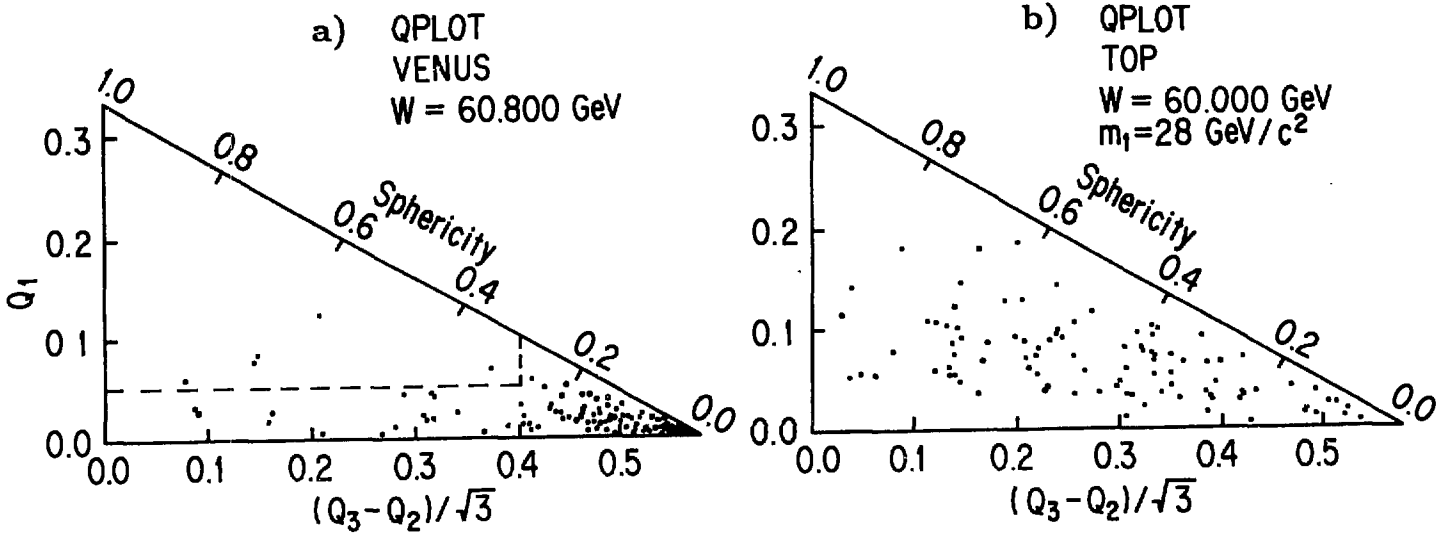
a) QPLOT
VENUS
W = 60.800 GeV
b) QPLOT
TOP
W = 60.000 GeV
m1=28 GeV/c2
Sphericity
1.0
0.8
0.6
0.4
0.2
0.0
Q1
(Q3-Q2)/√3
0.0
0.1
0.2
0.3
0.4
0.5

Fig.2

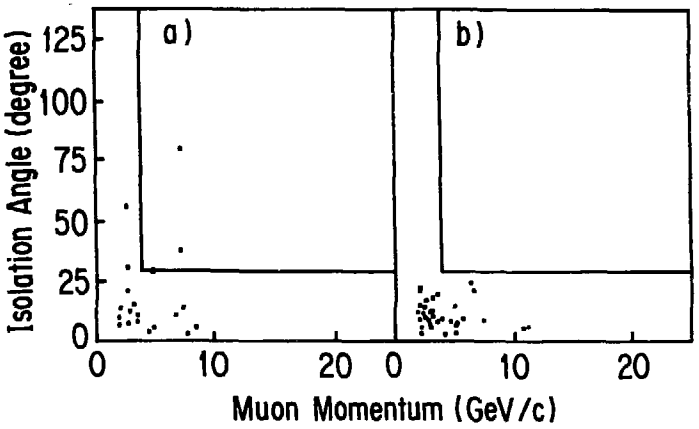

Fig.3

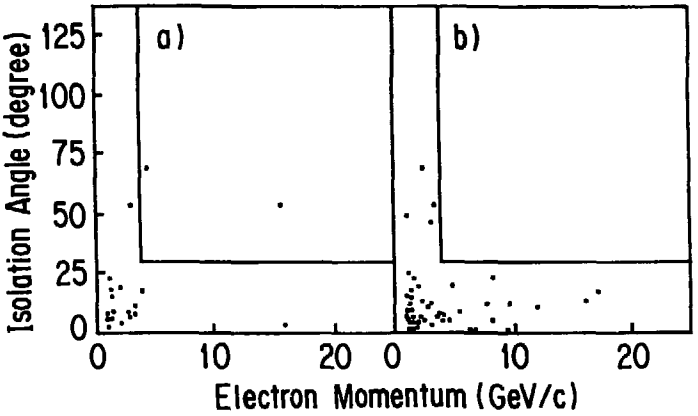

Fig.4

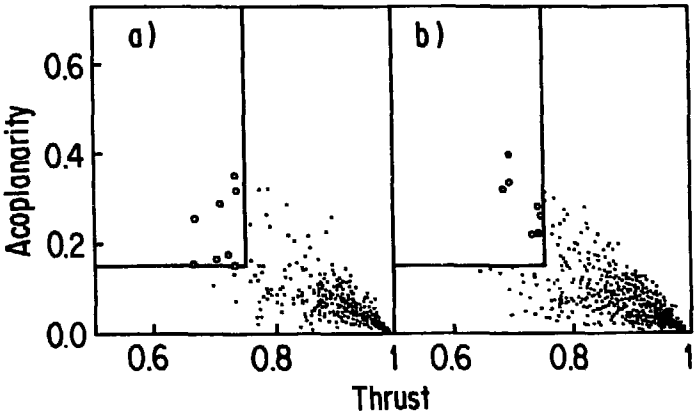

Fig.5

Fig.6

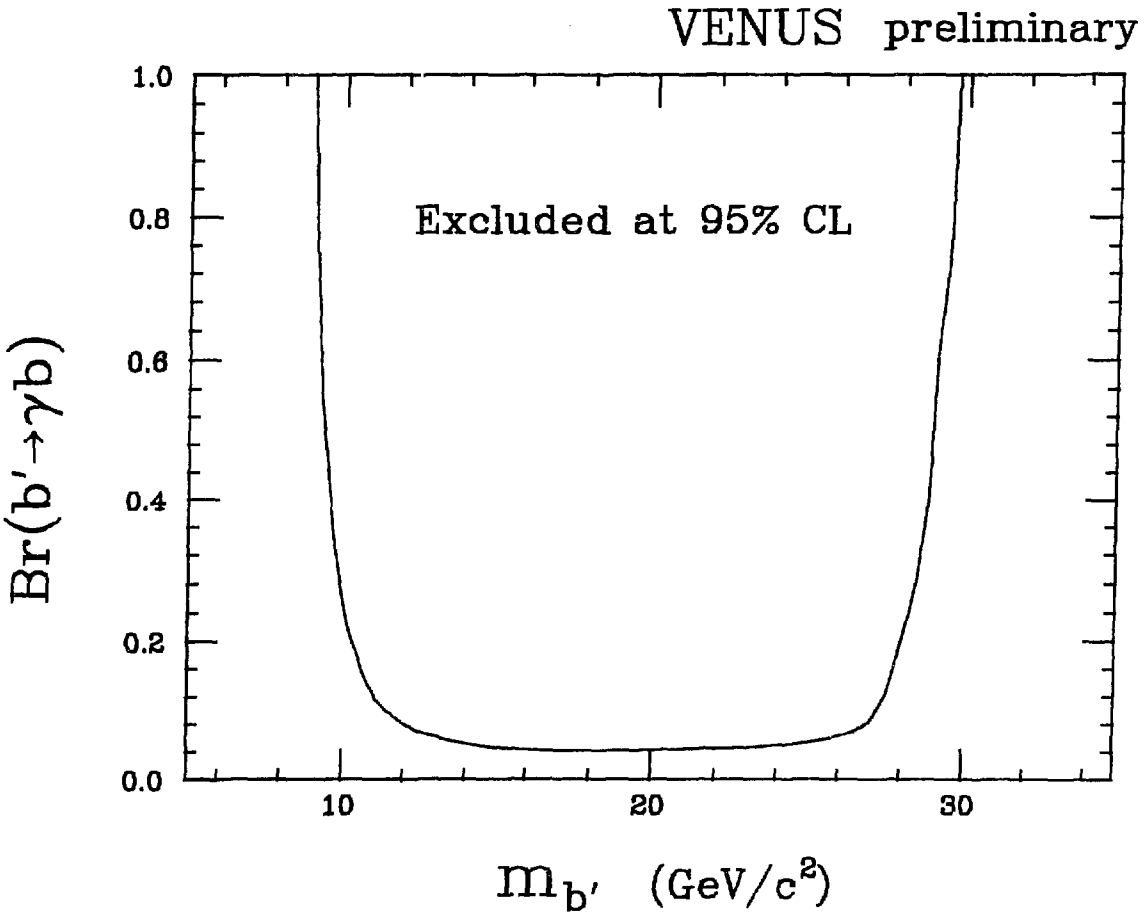
VENUS preliminary
Excluded at 95% CL
Br(b'→γb)
1.0
0.8
0.6
0.4
0.2
0.0
10
20
30
m_b' (GeV/c²)

Fig.7

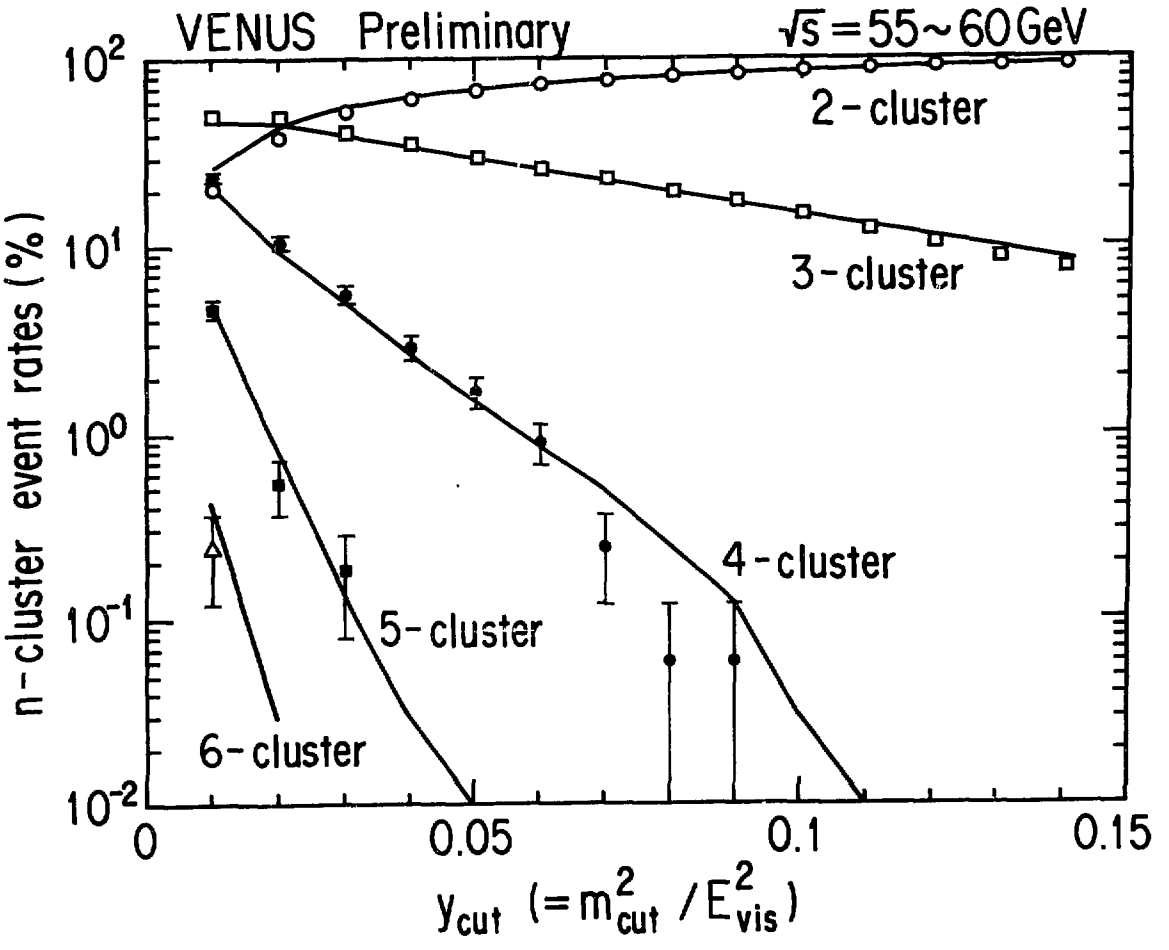
VENUS Preliminary
√s = 55~60 GeV
2-cluster
3-cluster
4-cluster
5-cluster
6-cluster
n-cluster event rates (%)
10²
10¹
10⁰
10⁻¹
10⁻²
0
0.05
0.1
0.15
y_cut (= m²_cut / E²_vis)

Fig.8

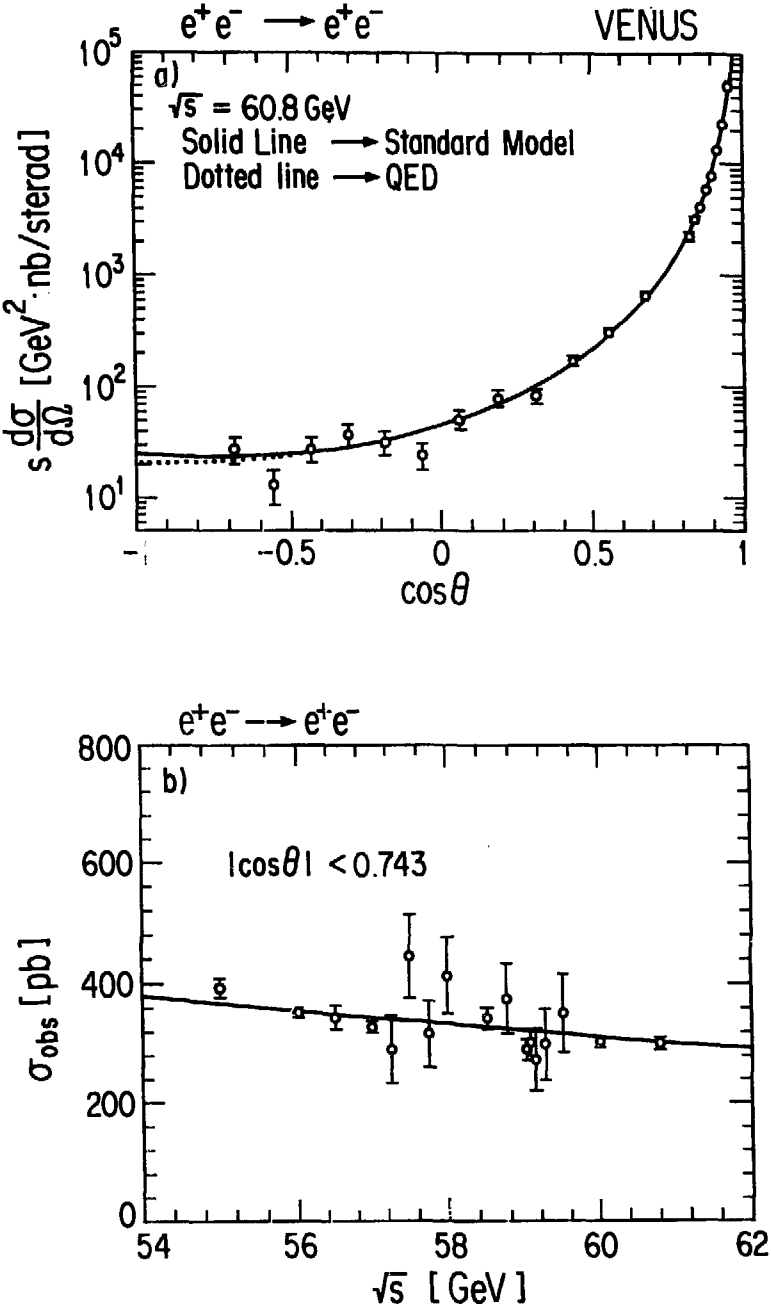
e+e− → e+e−
VENUS
a)
√s = 60.8 GeV
Solid Line → Standard Model
Dotted line → QED
s dσ/dΩ [GeV2·nb/sterad]
cosθ
e+e− → e+e−
b)
|cosθ| < 0.743
σobs [pb]
√s [GeV]

Fig.9

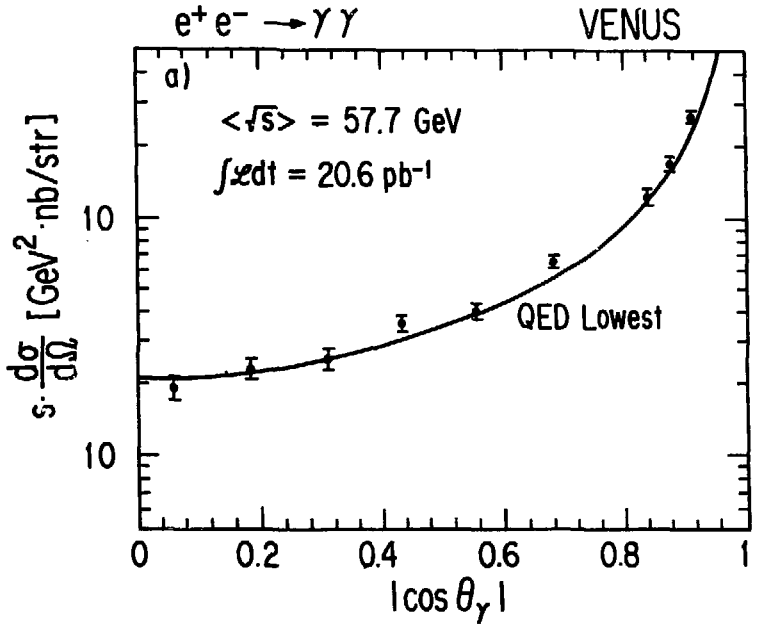
e+ e− → γ γ
VENUS
a)
<√s> = 57.7 GeV
∫£dt = 20.6 pb-1
QED Lowest
s·dσ/dΩ [GeV2·nb/str]
10
10
0
0.2
0.4
0.6
0.8
1
|cos θγ|

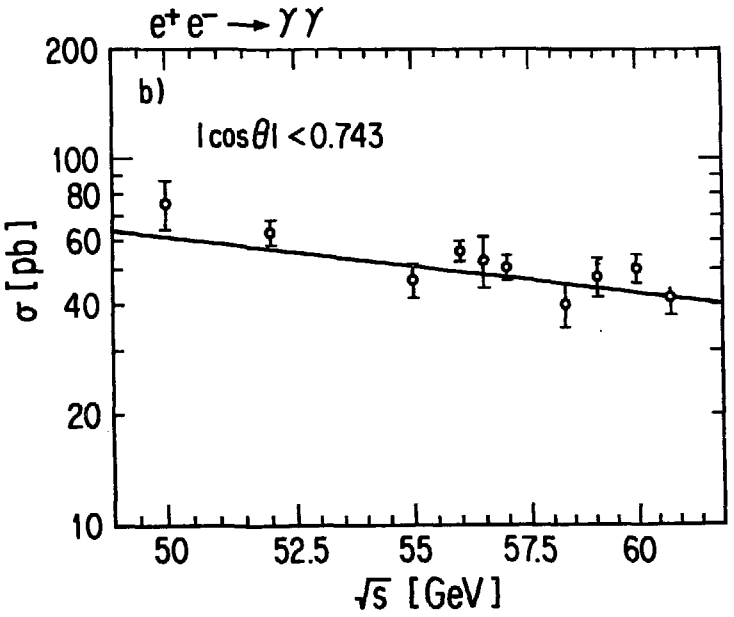
e+ e− → γ γ
b)
|cosθ| <0.743
σ [pb]
200
100
80
60
40
20
10
50
52.5
55
57.5
60
√s [GeV]

Fig.10

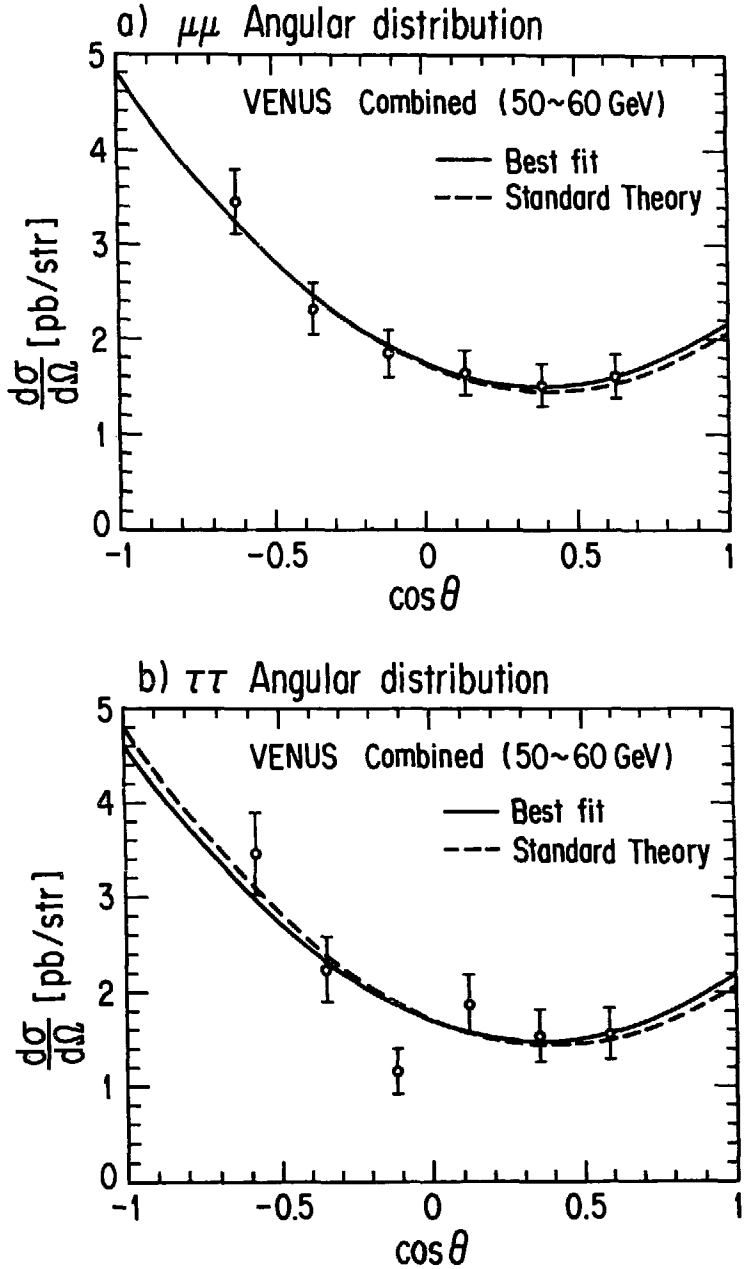
a) μμ Angular distribution
VENUS Combined (50~60 GeV)
Best fit
Standard Theory
dσ/dΩ [pb/str]
cosθ
b) ττ Angular distribution
VENUS Combined (50~60 GeV)
Best fit
Standard Theory
dσ/dΩ [pb/str]
cosθ

Fig.11

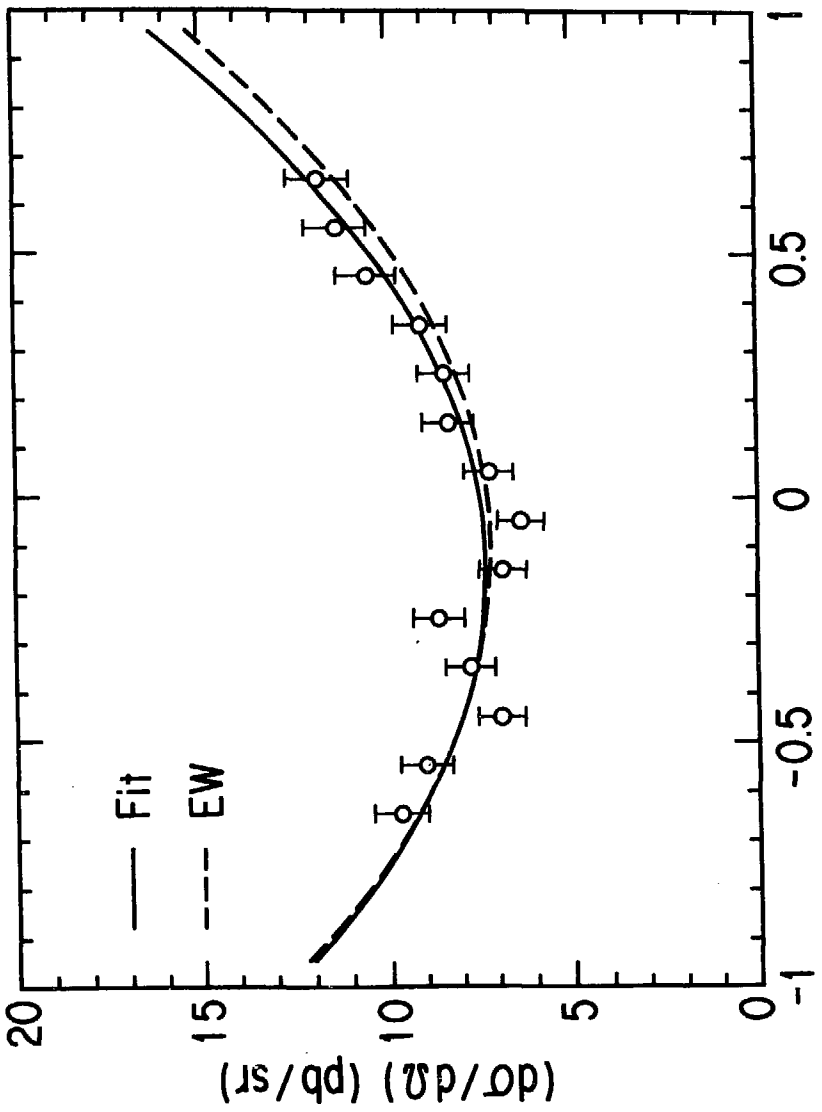

Fig.12

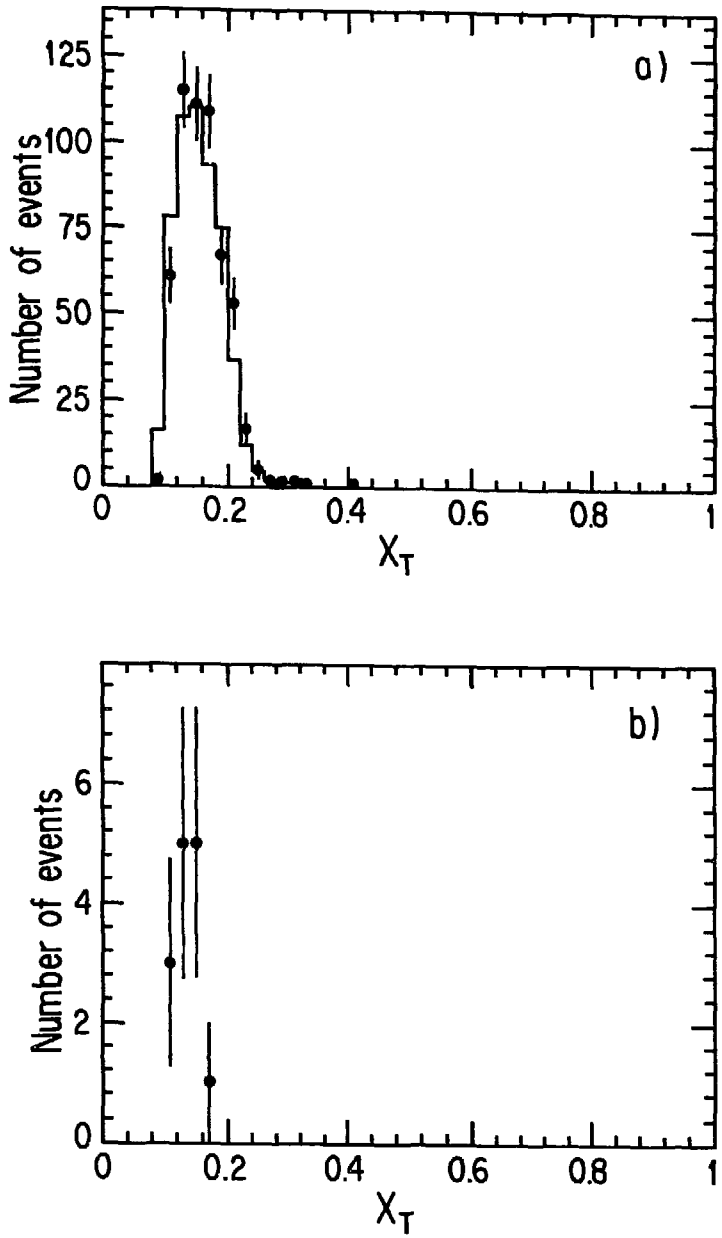
a)
Number of events
125
100
75
50
25
0
0
0.2
0.4
0.6
0.8
1
X_T
b)
Number of events
6
4
2
0
0
0.2
0.4
0.6
0.8
1
X_T

Fig.13